A Toy Model for Polymerization Dynamics and Molecular Weight Distribution

Jingdan Chen*

Department of Chemistry, University of Illinois at Urbana-Champaign, Urbana, IL 61801, United States

E-mail: jingdan2@illinois.edu

Abstract

Precise control over molecular weight distribution (MWD) in polymers is crucial for tailoring material properties across various applications, while understanding the underlying polymerization dynamics is essential for achieving this control. This project develops a finite-difference kinetic simulation framework to model polymerization dynamics and resulting MWD. The model incorporates key elementary reactions including initiation, propagation, chain transfer, and termination. The investigation examines chemical factors such as the combination-disproportionation ratio for termination and chain-length dependent propagation rates, alongside physical factors like diffusion control. Results demonstrate that MWD and conversion dynamics in radical bulk polymerization emerge from the complex mutual interactions between these chemical and physical parameters. This simulation framework provides a useful tool for explaining and predicting kinetic behavior in radical polymerization.

Keywords

Radical Polymerization, Molecular Weight Distribution, Finite-Difference Modeling

Introduction

Polymer products are widely acknowledged within the scientific community as complex mixtures with varying compositions and microstructures. The molecular weight distributions (MWD), or chain-length distributions (CLD) of polymers play a crucial role in determining their chemical and physical properties. Parameters such as average molecular weight (e.g., number-averaged molecular weight M_n, weight-average molecular weight M_w, and Z-average molecular weight) and polydispersity index (PDI, Đ) are commonly used to characterize MWD, as illustrated in equation 1 and 2, providing statistical measures of central tendency and dispersion. In addition to these parameters, other factors like asymmetry factor (A_s), skewness factor, and kurtosis factor are employed to offer detailed statistical descriptions of MWD.[1] The manipulability of MWD during the synthesis process has been demonstrated to result in a diverse range of physical properties in polymer products. For instance, Kottisch et al. customized the initiator injection rate curve during anionic styrene polymerization to produce polymers with similar average molecular weight and polydispersity index but distinct asymmetry factors. Variations in Young's modulus and viscosity were observed in different samples.[2] Computational methods for simulating MWD play a crucial role in interpreting experimental data and predicting MWD outcomes in advance. These methods are valuable for investigating mechanisms, facilitating discoveries, and guiding the design of MWD.

$$\begin{aligned} M_n &= \frac{\sum M_i N_i}{\sum N_i} \\ M_w &= \frac{\sum M_i^2 N_i}{\sum M_i N_i} \end{aligned} \tag{1}$$

$$Đ = \frac{M_w}{M_n} = \frac{\sigma}{M_n^2} + 1 \tag{2}$$

There have been numerous endeavors aimed at forecasting MDW using kinetic models, from simulation efforts like Monte Carlo[3] chain growth simulation to analytical solution

provided by Markov-chain model[4] or steady-state model (*i.e.* Flory distribution). In cases where only terminal effects are taken into account, the polymerization process can be viewed as a Markov-chain model. In this model, the distribution of chain lengths can be effectively determined based on the probabilities of chain termination and propagation, with their combined probabilities assumed to total unity. Consider the scenario involving termination by disproportionation or chain transfer, excluding combination reactions. The number-fraction ($\underline{N}_x$), weight-fraction (w_x), number- and weight-average molecular weight (M_n, M_w), and dispersity index (Đ) can be determined using equation 3 with the probability of propagation denoted by p as shown in equation 4. Here, r_p, r_t, and r_{tr} represent the rates of propagation, termination by disproportionation, and chain transfer, respectively. In the case where combinatorial termination (with a rate of r_{tc}) is involved, the weight distribution and the value of p can be adjusted accordingly as described by equation 5. The parameter A represents the fraction of polymer molecules generated through disproportionation and chain transfer reactions[4,5]

$$\begin{aligned} \underline{N}_x &= (1-p)p^{x-1} \\ w_x &= x(1-p)^2p^{x-1} \\ M_n &= \frac{1}{(1-p)} \\ M_w &= \frac{(1+p)}{(1-p)} \\ Đ &= \frac{M_w}{M_n} = (1+p) \end{aligned} \tag{3}$$

$$p = \frac{r_p}{r_p + r_t + r_{tr}} \tag{4}$$

$$\begin{aligned} \underline{N}_x &= A(1-p)p^{x-1} + \frac{1}{2}(1-A)(1-p)^2(x-1)p^{x-2} \\ w_x &= Ax(1-p)^2p^{x-1} + \frac{1}{2}(1-A)x(1-p)^3(x-1)p^{x-2} \\ p &= \frac{r_p}{r_p + r_{td} + r_{tr} + r_{tc}} \end{aligned} \tag{5}$$

The fundamental concept of the Flory distribution revolves around a steady-state assumption concerning all radical species or living polymers with active radical terminals (as opposed to dead polymers where no reactive radical exists) within a continuous stirred tank reactor with an average residence time t_r.[6] The classical Flory distribution primarily considers initiation, propagation, and disproportionate deactivation. The resulting number-fraction and weight fraction are presented in equation 6 with τ defined in equation 7. The Extended Flory distribution in free radical polymerization with combinational termination in a batch reactor can be derived correspondingly by determining the number-fraction and weight fraction of radical species (referred to as living polymers) with a scaling relationship similar to that in equation 6, relative to τ as defined in equation 9. Here, $[M]$ represents the concentration of unreacted monomer, and $[P_x^*]$ denotes the concentration of living polymer with a degree of polymerization equal to x. However, for polymer chains (referred to as dead polymers), the distribution is influenced by the nature of combinational reactions, as expressed in equation 8.

$$\begin{aligned} \underline{N}_x &= \tau e^{-x\tau} \\ w_x &= \tau^2 x e^{-x\tau} \end{aligned} \tag{6}$$

$$\tau = \frac{k_d + \frac{1}{t_r}}{k_p[M]} \tag{7}$$

$$\begin{aligned} \underline{N}_{x,dead} &= \frac{k_{td}(\tau e^{-x\tau}) + \frac{k_{tc}}{2}\tau^2 x e^{-x\tau}}{k_{td} + \frac{k_{tc}}{2}} \\ w_x &= \frac{k_{td}(\tau^2 x e^{-x\tau}) + \frac{k_{tc}}{2}(\tau^3 x^2 e^{-x\tau})}{k_{td} + \frac{k_{tc}}{2}} \end{aligned} \tag{8}$$

$$\tau = \frac{k_t \cdot \sum_{x=0}^{\infty}[P_x^*]}{k_p[M]} \tag{9}$$

In this study, we employ a finite-difference approach, utilizing a finite element time step in conjunction with a parameterized elementary reaction network to monitor the concentra-

tion changes of various species, such as monomers, initiators, polymers, and radical species with varying degrees of polymerization in our system in radical bulk polymerization. This methodology is applied to simulate the kinetics of conversion and the distribution of molecular weights. The obtained results are qualitatively assessed against experimental data and the previously mentioned analytical solutions, namely the Flory distribution and the Markov chain model. An ablation study, comparing the kinetic performance with and without specific physical and chemical factors, is conducted to demonstrate their influence on conversion and MDW.

Methods

Polymerization Mechanism

Initiation is conventionally understood to be triggered by initiators, for example, AIBN and BPO. These initiators typically possess labile covalent bonds that are susceptible to heat and light. Upon spontaneous decomposition, these initiators generate initiator radicals, which then attack monomer molecules, thereby commencing chain growth (propagation), see equation 10. For the sake of simplicity, the chemical initiation step, which generates radical species capable of initiating polymerization (considered to have a polymerization degree of 1), can be represented by an effective kinetic constant, as illustrated in equation 11.

$$\begin{aligned} \mathrm{I} &\xrightarrow{\mathrm{k_i}} 2\mathrm{R_i^*} \\ \mathrm{R_i^*} + \mathrm{M} &\xrightarrow{\mathrm{k_{p0}}} \mathrm{R_1^*} \end{aligned} \tag{10}$$

$$\mathrm{I_{\frac{1}{2}}} + \mathrm{M} \xrightarrow{\mathrm{k_i}'} \mathrm{R_1^*} \tag{11}$$

The kinetics of monomer and initiator consumption, as well as radical generation, can be distinguished by the initiator efficiency (f), which represents the fraction of initiator decompositions that lead to the formation of initiating radicals.

$$
\begin{aligned}
\left[\mathrm{I}_{\frac{1}{2}}\right] &= 2\,[\mathrm{I}] \\
\mathrm{k_i} &= 2\mathrm{k_i}' \\
\frac{d\left[\mathrm{I}_{\frac{1}{2}}\right]}{dt}_{\mathrm{ini}} &= -\mathrm{k_i}'\left[\mathrm{I}_{\frac{1}{2}}\right][\mathrm{M}] \\
\frac{d\,[\mathrm{R_1}^*]}{dt}_{\mathrm{ini}} &= -\frac{d\,[\mathrm{M}]}{dt}_{\mathrm{ini}} = \mathrm{k_i}'\mathrm{f}\left[\mathrm{I}_{\frac{1}{2}}\right][\mathrm{M}]\ \ (1 > \mathrm{f} > 0)
\end{aligned}
\tag{12}
$$

Monomers can also undergo activation by light or heat, even in the absence of an added chemical initiator. While the rate of self-initiation is generally negligible compared to initiation via added initiators due to the lack of inherent weak bonds in the monomer structure, it can become significant for certain monomers above specific temperatures. For instance, styrene exhibits significant self-initiation at temperatures exceeding $120\,^{\circ}C$, proceeding through a Diels-Alder reaction mechanism.[7] Although the specific form of the kinetic equation varies depending on the initiation mechanism, for the sake of simplicity and generalizability, we can assume the exponents x and y in equation 13 to be either 1 or 2. The molecular weight distribution is closely related to the concentration of propagating radicals, which is, in turn, influenced by the initiation step. Generally, maintaining a low but steady concentration of radicals tends to favor the formation of higher molecular weight polymers.

$$
\mathrm{xM} \xrightarrow{\mathrm{k_{it}}} \mathrm{yR_1^*} \tag{13}
$$

Following initiation, chain propagation occurs through the reaction between all existing radical species in the system and monomer molecules. Conversely, depolymerization, which leads to chain shortening, can become significant at elevated temperatures. Given the temperature and reaction enthalpy, the kinetic constant for depolymerization can be estimated by applying the Arrhenius equation and transition state theory, as shown in equation 15.

$$
\begin{aligned}
\mathrm{R_i^* + M} &\xrightarrow{\mathrm{k_p}} \mathrm{R_{i+1}^*}\ \ (\mathrm{i} \geq 1) \\
\mathrm{R_{i+1}^*} &\xrightarrow{\bar{\mathrm{k}}_{\mathrm{p}}} \mathrm{R_i^* + M}
\end{aligned}
\tag{14}
$$

$$\ln \frac{k_p}{\bar{k}_p} = -\frac{\Delta H}{RT} \tag{15}$$

Chain transfer reactions can occur not only between radical species and small molecules such as solvent, monomer, and polymerization retarder, but also with existing oligomer or polymer molecules within the system. Generally, chain transfer to small molecules tends to decrease the molecular weight by terminating a growing polymer chain and initiating a new one on the small molecule. Conversely, chain transfer to existing polymer chains can lead to branching in the polymer structure, potentially influencing the overall molecular weight distribution and properties.

$$\mathrm{R_i^* + M \xrightarrow{k_{fm}} P_i^* + R_1^*} \tag{16}$$

In the later stages of the reaction, as the radical concentration increases and the monomer concentration decreases, termination becomes the predominant fate of the radical species. This step halts chain growth, resulting in the formation of stable polymer molecules through the reaction of two radicals, either by combination or disproportionation. In most systems, conbinational termination is dominant.[8]

$$\begin{aligned} &\mathrm{R_i^* + R_j^* \xrightarrow{k_{tc}} P_{i+j}\ (combination)} \\ &\mathrm{R_i^* + R_j^* \xrightarrow{k_{td}} P_i + P_j\ (disproportionation)} \end{aligned} \tag{17}$$

By considering these fundamental mechanisms, we can model the instantaneous changes in concentration for all species within the system. This includes the concentrations of the chemical initiator, monomer, radicals with varying degrees of polymerization, and dead polymer chains of different lengths. These changes are governed by the five elementary reactions previously discussed, and their rates can be expressed using the corresponding kinetic constants and the concentrations of the reacting species. The rest of definitions of all kinetic constants and concentration terms can be found in supplementary information.

$$
\begin{aligned}
\frac{d\left[\mathrm{M}\right]}{dt} &= \frac{d\left[\mathrm{P_1}\right]}{dt} - \mathrm{k_p}\left[\mathrm{M}\right]\sum_{\mathrm{i=1}}^{\mathrm{n_{max}}}\left[\mathrm{R_i}^*\right] - \mathrm{k_i}'\mathrm{f}\left[\mathrm{I}\right]\left[\mathrm{M}\right] - \mathrm{xk_{it}}\left[\mathrm{M}\right]^{\mathrm{x}} \\
&\quad + \bar{\mathrm{k}}_{\mathrm{p}}\sum_{\mathrm{i=2}}^{\mathrm{n_{max}}}\left[\mathrm{R_i}^*\right] - \mathrm{k_{fm}}\left[\mathrm{M}\right]\sum_{\mathrm{i=1}}^{\mathrm{n_{max}}}\left[\mathrm{R_i}^*\right] \\
\frac{d\left[R_i^*\right]}{dt} &= k_p\left[M\right]\left(\left[{R_{i-1}}^*\right] - \left[{R_i}^*\right]\right) + \bar{k}_p\left(\left[{R_{i+1}}^*\right] - \left[{R_i}^*\right]\right) \\
&\quad + \left(k_{tc} + k_{td}\right)\left(\sum_{j=1}^{n_{max}}\left[{R_i}^*\right]\left[{R_j}^*\right] + \left[{R_i}^*\right]^2\right) - k_{fm}\left[M\right]\left[{R_i}^*\right] \;\; (i > 1) \\
\frac{d\left[{R_1}^*\right]}{dt} &= k_i'\mathrm{f}\left[M\right]\left[\mathrm{I}_{\frac{1}{2}}\right] + \mathrm{k_{it}y}\left[\mathrm{M}\right]^{\mathrm{x}} - \mathrm{k_p}\left[\mathrm{M}\right]\left[{\mathrm{R}_1}^*\right] + \bar{k}_p\left[{\mathrm{R}_2}^*\right] \\
&\quad + \left(\mathrm{k_{tc}} + \mathrm{k_{td}}\right)\left(\sum_{j=1}^{n_{max}}\left[{R_1}^*\right]\left[{R_j}^*\right] + \left[{R_1}^*\right]^2\right) + \mathrm{k_{fm}}\sum_{j=2}^{n_{max}}\left[{R_\mathrm{j}}^*\right]\left[\mathrm{M}\right] \\
\frac{d\left[\mathrm{P_i}\right]}{dt} &= \mathrm{k_{td}}\left[{\mathrm{R_i}}^*\right]\sum_{\mathrm{j=2}}^{n_{max}}\left[\mathrm{R_j}\right] + \mathrm{k_{fc}}\sum_{\mathrm{j=1}}^{\mathrm{i-1}}\left[{\mathrm{R_{i-j}}}^*\right]\left[{\mathrm{R_j}}^*\right] \;\; (\mathrm{i} > 1)
\end{aligned}
\tag{18}
$$

Simulation

All simulations are conducted using a finite-difference time step of $\Delta t = 10^{-6}$ min, starting from an initial $\Delta t_0 = 10^{-10}$ min over approximately 700 steps for the system to stabilize. The simulation temperature is maintained at 120 °C, with the initial concentration of AIBN as the initiator set at 0.02 M. Incorporating combinational termination poses challenges due to its higher computational complexity (approximately $O(N^2)$ as shown in Equation 18), resulting in shorter simulations (achieving less than 50% monomer conversion). This study does not employ advanced integrators, hence concentrations of any species are determined by the relationship described in Equation 19.

$$
[X]_{t+1} = [X]_t + \Delta t \cdot \frac{d[X]_t}{dt} \tag{19}
$$

Results and Discussion

Although combinational termination is considered dominant in most cases, introducing combinational termination would significantly slow down the simulation due to its higher complexity. Thus, the simulation of styrene (Sty) polymerization without combinational termination is first conducted with results depicted in Fig. 1, with corresponding experimental outcomes presented in Fig. 2(A) and Fig. 2(B) for comparison. Interestingly, the experimental observations reveal a self-acceleration phenomenon at around 50% conversion, a behavior not replicated in our simulation. Furthermore, the cumulative degree of polymerization (D_p) and radical concentration appear relatively constant shortly after initiation, giving a solid bedrock to the assumption of steady-state conditions in the Flory distribution theory. Chain length distribution from our simulation is sigmoid-shape decaying curve, being inconsistent with Poison-like distribution which was measured from experiments.

To address the discrepancy between the conversion kinetics and the CLD observed in simulations and experimental data, we reintroduced combinational termination into our model. The CLD outcomes obtained from the Markov-chain model, Flory distribution theory, and our simulation incorporating combinational termination are illustrated in Fig. 3(A) and Fig. 3(B). The results from the Markov-chain model and Flory distribution exhibit significant overlap, while our simulation also closely mirrors these outcomes. All three approaches demonstrate good agreement with the experimentally determined MDW and CLD profile. Hence, these computational methods effectively replicate the CLD and MDW characteristics of the poly-styrene (PSty) system, underscoring the importance of combinational termination in shaping the CLD.

To demonstrate the applicability of the three computational approaches in predicting Chain Length Distribution (CLD) and Molecular Weight Distribution (MWD), we conducted additional testing using a poly-methyl methacrylate (PMMA) radical bulk polymerization system. All three methods account for combinational termination. The outcomes are illustrated in Fig. 3(C) and Fig. 3(D), alongside the corresponding experimental results

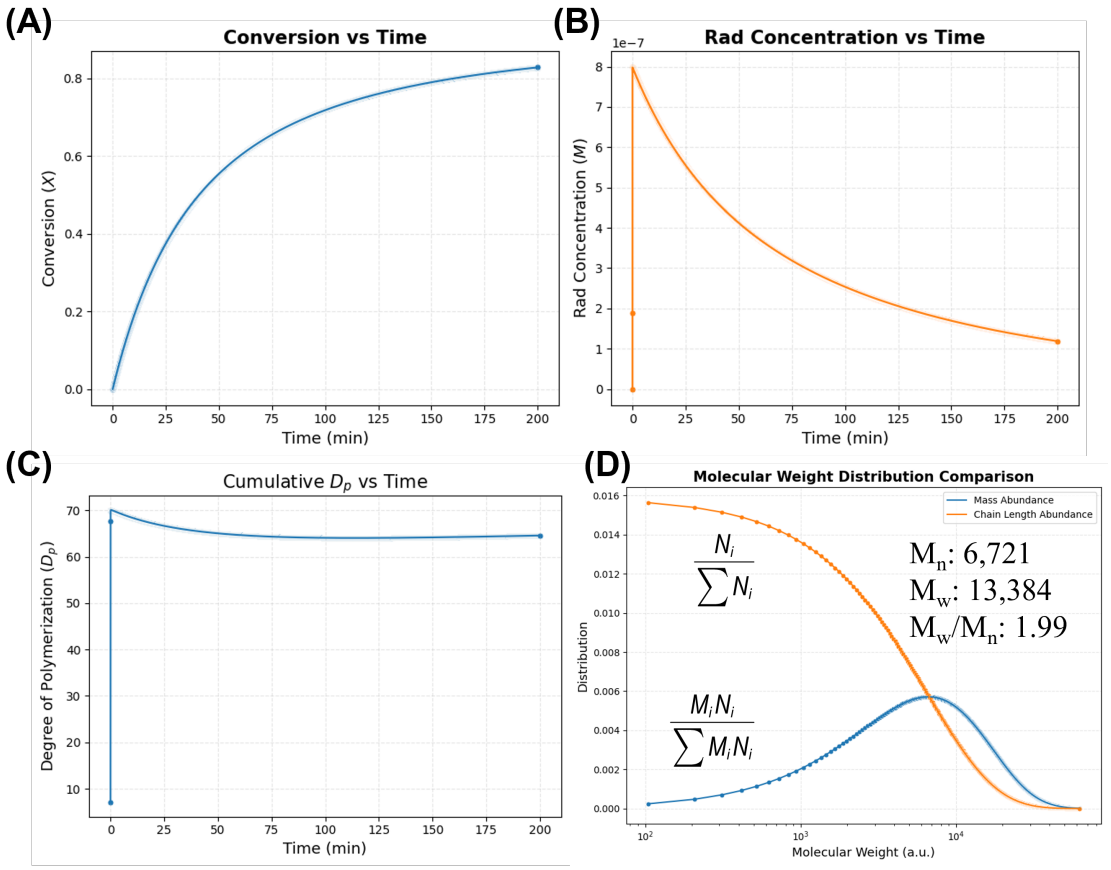

Figure 1: Styrene polymerization without combinational termination. (A) Monomer conversion evolution over time. (B) Radical (active polymer) concentration evolution over time. (C) Cumulative degree of polymerization change over time. (D) Cumulative CLD and MWD at the end of simulation.

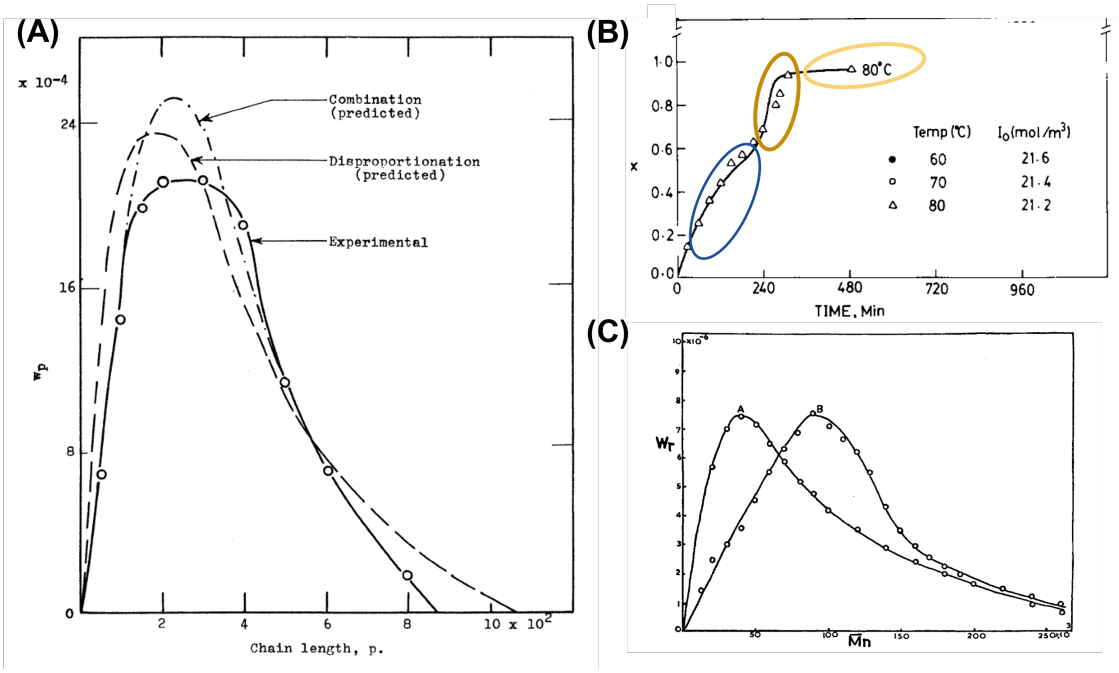

Figure 2: Experimental result for styrene (Sty) and methyl methacrylate (MMA) polymerization from literature. (A) Cumulative CLD of poly-styrene.[9] (B) Monomer conversion evolution over time of poly-styrene.[10] (C) Cumulative CLD of poly-styrene, A and B are different samples from different experimental channel.[11]

presented in Fig. 2(C) for comparison. Despite considering appropriate termination mechanisms, the CLD for PMMA reverts to a sigmoid-like decay curve. The analysis reveals a more pronounced chain-length-dependent decay of the propagation rate constant (k_p) in the Methyl Methacrylate (MMA) system compared to Styrene (Sty).[12] As the polymerization progresses, longer polymer chains are more likely to undergo intramolecular termination, leading to a reduced apparent monomer concentration around them, consequently resulting in a decay of k_p as depicted in Fig. 4(A). Upon appropriately integrating the decay of k_p into our simulations, the simulation outcomes, as demonstrated in Fig. 4(B), exhibit a Poisson-like distribution of CLD, in agreement with experimental observations. This underscores that, in addition to combinational termination, the chain-length-dependent behavior of k_p significantly influences the shape of the CLD curve in the PMMA system.

The final question to be addressed pertains to the origin of self-acceleration, commonly referred to as the gel and glassy effect, observed during experimental investigations of con-

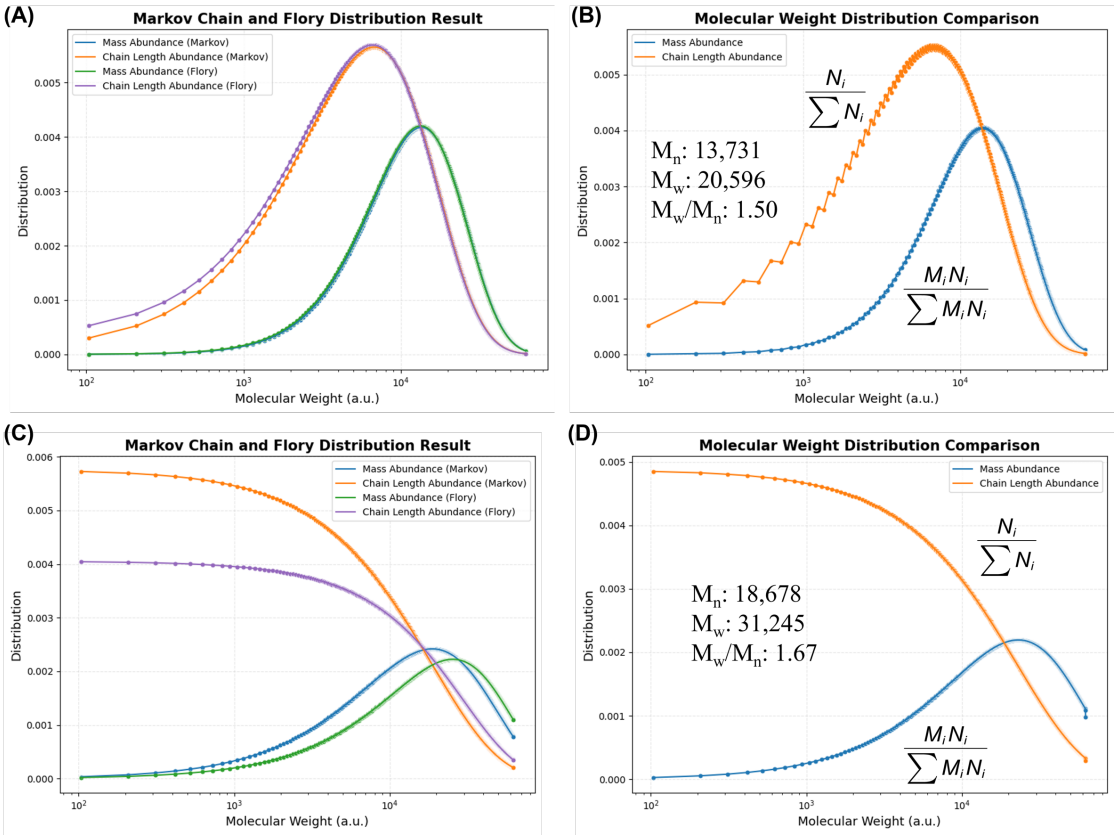

Figure 3: Comparing CLD and MWD result between Markov-chain model, Flory distribution and our simulation result with combinational termination taken into consideration. (A) Markov-chain model and Flory distribution for poly-Sty. (B) Simulation result for poly-Sty. (C) Markov-chain model and Flory distribution for poly-MMA. (D) Simulation result for poly-MMA.

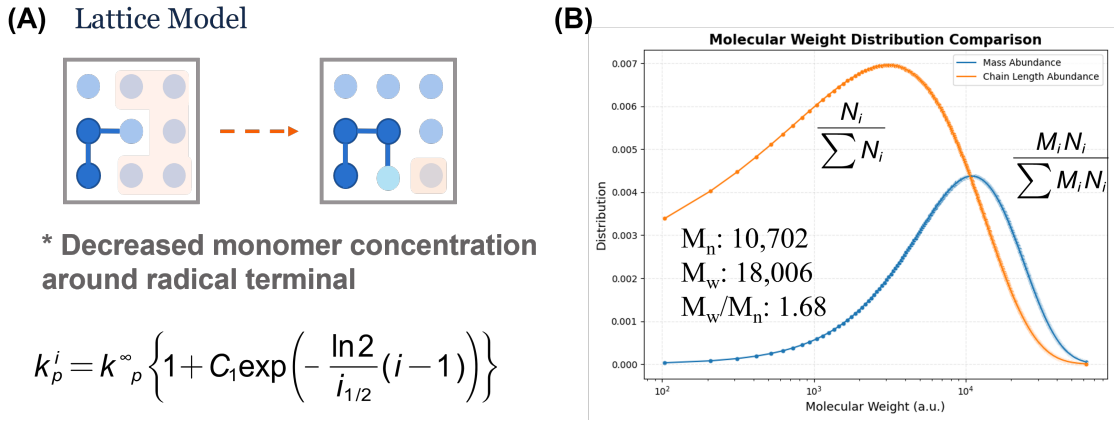

Figure 4: Chain-length dependent propagation rate (k_p) in MMA polymerization. (A) Sketch of using lattice model to explain the origin of chain-length dependent decay of k_p in PMMA. (B) Cumulative CLD of PMMA with both combinational termination and k_p decay into consideration.

centrated solution (or bulk) polymerization systems. The Free Volume Theory[8] provides a plausible explanation for this phenomenon by attributing it to varying diffusion controls at different stages of polymerization. According to the theory, a termination reaction involves three diffusion steps: translational diffusion, segmental diffusion, and chemical reaction diffusion, as illustrated in Figure 5. Translational diffusion describes the movement of two active polymer chains through the solution until they come into contact. Segmental diffusion involves the entanglement of the encountering polymer chains, leading to the proximity of their radical terminals. Reaction diffusion entails the continuous growth of the radical terminals by interacting with surrounding monomers and ultimately approaching each other. Furthermore, the Free Volume Theory suggests that the kinetic constant of termination is influenced by the distinct diffusion processes occurring at each stage. When the free volume in the system is lower than critical free volume, translational diffusion is largely damping the overall termination, giving higher radical concentration and self-accelerated monomer transformation in the system.

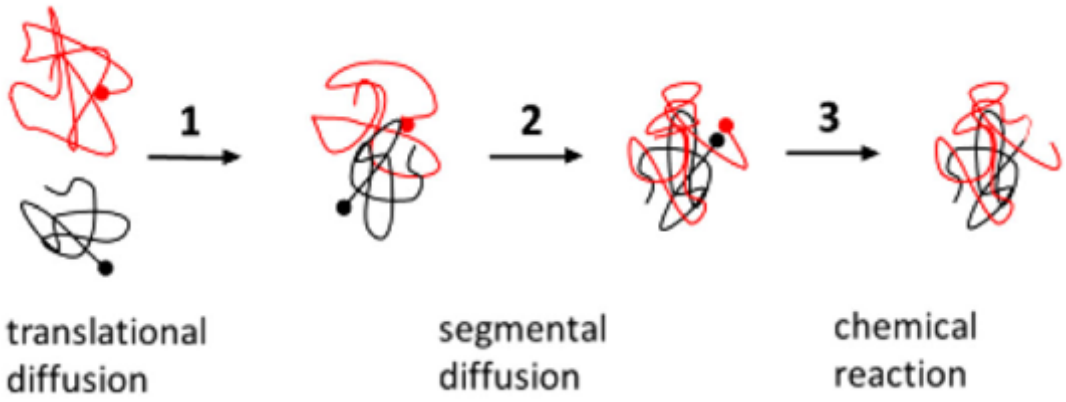

Figure 5: Three steps for termination reaction: translational diffusion, segmental diffusion and chemical reaction (diffusion).[13]

After considering a change in the termination rate constant near the critical point in our simulation, we did not observe self-acceleration, as depicted in Fig. 6(A). The radical concentration and degree of polymerization showed an upward trend, illustrated in Fig. 6(B) and 6(C). Additionally, the first derivative of the conversion-over-time curve was plotted in

Fig. 6(D), revealing the emergence of a shifting point in this simulation. Consequently, by appropriately parameterizing the free volume theory, we anticipate that self-acceleration could be observed and effectively explained in our simulation.

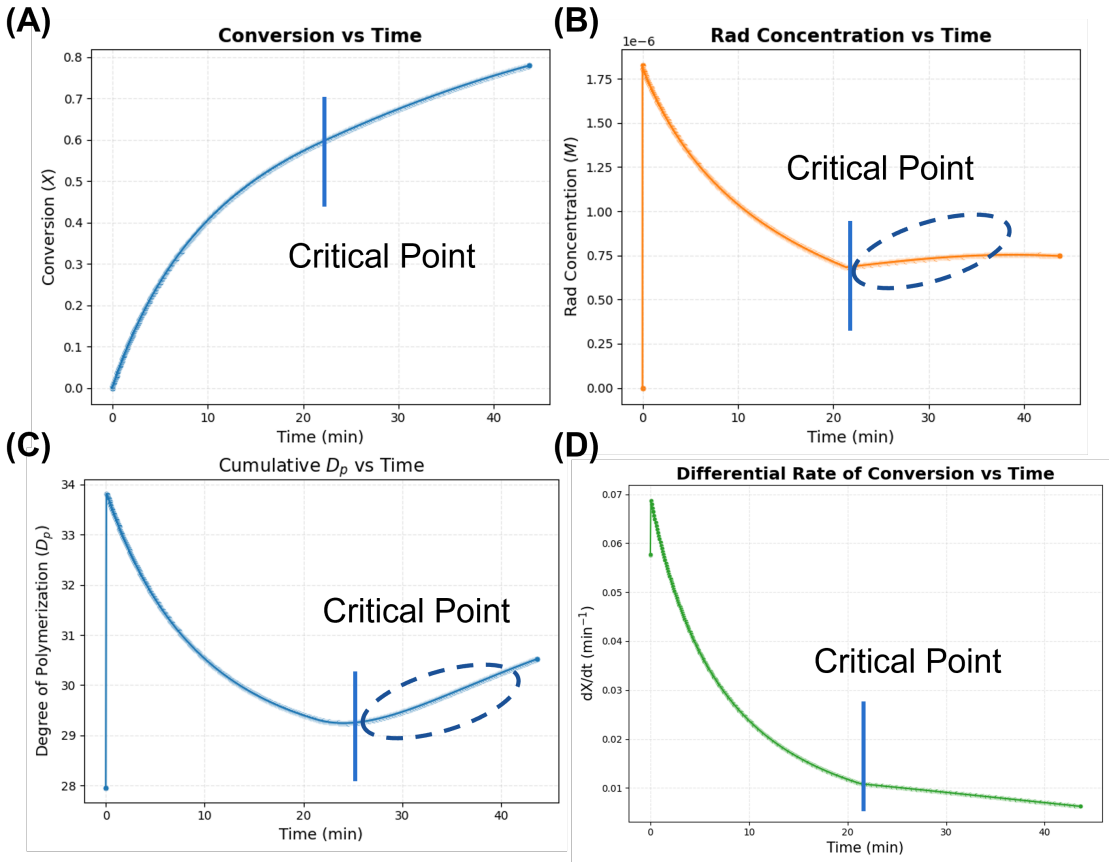

Figure 6: Simulation of polymerization of Sty, with incorporation of free volume theory. (Simulation is under $[AIBN] = 0.05M, T = 100.0\,^{\circ}C$) (A) Conversion of monomer change over time. (B) Radical (active polymer) concentration evolution over time. (C) Cumulative degree of polymerization change over time. (D) Derivation of conversion over time curve.

Conclusion

In conclusion, we have formulated a simplified model to analyze the distribution of molecular weight and chain length in radical bulk polymerization. Through detailed testing on methyl methacrylate and styrene systems, our model demonstrates a strong correlation with the Flory distribution theory and findings obtained from a Markov-chain model applied to the

case of styrene's chain length distribution and molecular weight distribution. Furthermore, our simulation effectively elucidates the phenomenon of self-acceleration in condensed polymerization by incorporating the free volume theory, thus shedding light on the underlying mechanisms of this behavior.

Acknowledgement

The author thanks teaching assistant of this class, James F. Tallman for having constructive discussion on the project. The author also thanks the instructor, Professor Antonia Statt and other classmates reviews for providing insightful advice for manuscript writing.

References

(1) Gentekos, D. T.; Sifri, R. J.; Fors, B. P. Controlling Polymer Properties through the Shape of the Molecular-Weight Distribution. *Nature Reviews Materials* **2019**, *4*, 761–774.

(2) Kottisch, V.; Gentekos, D. T.; Fors, B. P. "Shaping" the Future of Molecular Weight Distributions in Anionic Polymerization. *ACS Macro Letters* **2016**, *5*, 796–800.

(3) Mavrantzas, V. G. Using Monte Carlo to Simulate Complex Polymer Systems: Recent Progress and Outlook. *Frontiers in Physics* **2021**, *9*, 661367.

(4) Odian, G. G. *Principles of Polymerization*, 4th ed.; Wiley-Interscience: Hoboken, N.J, 2004; pp 289–292.

(5) Smith, W. B.; May, J. A.; Kim, C. W. Polymer Studies by Gel Permeation Chromatography. *Journal of Polymer Science Part A-2: Polymer Physics* **1966**, *4*, 365–374.

(6) Jiao, S.; Liu, R.; Lin, X.; Chen, X. Analytical Expressions for Molecular Weight Distribution in Steady-State Radical Polymerizations. *Polymer* **2025**, *328*, 128427.

(7) Khuong, K. S.; Jones, W. H.; Pryor, W. A.; Houk, K. N. The Mechanism of the Self-Initiated Thermal Polymerization of Styrene. Theoretical Solution of a Classic Problem. *Journal of the American Chemical Society* **2005**, *127*, 1265–1277.

(8) Jung, W.; Riahinezhad, M.; Duever, T. A. Case Studies With Mathematical Modeling of Free-Radical Multi-Component Bulk/Solution Polymerization Part 1. *Journal of Macromolecular Science* **2017**, 339–371.

(9) Lei, G. Y. S. The Distribution of Molecular Weight in Polystyrene. *Electronic Theses and Dissertations.* **1965**, 6394.

(10) Kumar, V.; Gupta, S. K. Optimal Parameter Estimation for Methyl Methacrylate Polymerization. *Polymer* **1991**, *32*, 3233–3243.

(11) Olaj, O. F.; Vana, P.; Zoder, M. Chain Length Dependent Propagation Rate Coefficient Kp in Pulsed-Laser Polymerization: Variation with Temperature in the Bulk Polymerization of Styrene and Methyl Methacrylate. *Macromolecules* **2002**, *35*, 1208–1214.

(12) Heuts, J. P.; Russell, G. T. The Nature of the Chain-Length Dependence of the Propagation Rate Coefficient and Its Effect on the Kinetics of Free-Radical Polymerization. 1. Small-molecule Studies. *European Polymer Journal* **2006**, *42*, 3–20.

(13) Buback, M.; Russell, G. T. Detailed Analysis of Termination Kinetics in Radical Polymerization. *Polymer International* **2023**, *72*, 869–880.

(14) Dorschner, D. Case Studies with Mathematical Modeling of Free-Radical Multi-Component Bulk/Solution Polymerization: Part 2. *Journal of Macromolecular Science* **2017**, 339–371.

Supporting Information Available

Code for simulation and data analysis is compiled at `https://github.com/Jingdan-Chen/PolyPhys_toy_MDW`. Kinetic parameters used for simulation is cited from reference[8,14] and listed below in Table 1, 2 and 3.

Table 1: Kinetic Parameters for AIBN

Parameter	**Monomer**	**Value**	**Unit**	**Description**
M_w	General	164.21	g/mol	Initiator molecular weight
k_d	Styrene	$6.33 \times 10^{16} \exp(-3.0719 \times 10^4/RT)$	L/min	Decomposition rate constant
	General	$6.23 \times 10^{16} \exp(-3.0704 \times 10^4/RT)$	L/min	Decomposition rate constant
f	Styrene	0.6	-	Initiator efficiency
	General	$0.0247 \exp(-2166/RT)$	-	Initiator efficiency

* R, ideal gas constant, is in $cal \cdot mol^{-1} \cdot K^{-1}$; T, temperature, is in K

Table 2: Kinetic Constants for Styrene

Parameter	Value	Unit	Description
M_w	104.12	g/mol	Molecular weight of the monomer
T_{gm}	185	K	Glass transition temp. of the monomer
T_{gp}	378	K	Glass transition temperature of the polymer
C_{pm}	430	cal/kg/K	Heat capacity of the monomer
C_{pp}	400	cal/kg/K	Heat capacity of the polymer
ΔH	-17000	cal/mol	Heat of reaction
ρ_m	$0.924 - 0.000918 \times (T - 273.15)$	kg/L	Density of the monomer
ρ_p	$1.084 - 0.000605 \times (T - 273.15)$	kg/L	Density of the polymer
k_p	$1.302 \times 10^9 \exp(-7759.2/RT)$	L/mol/min	Rate of propagation
k_t	$4.92 \times 10^{11} \exp(-3471.3/RT)$	L/mol/min	Rate of termination
$k_{td,ratio}$	0.01	-	Disproportionation to combination ratio
k_{fm}	$1.386 \times 10^8 \exp(-12670/RT)$	L/mol/min	Transfer to monomer rate
k_{fp}	0	L/mol/min	Transfer to polymer rate
k_{pin}	0	L/mol/min	Internal double bond rate of propagation
k_{pte}	0	L/mol/min	Terminal double bond rate of propagation
Δ	0.001	L/g	Reaction radius for translational diffusion
V_{fc}	$0.31105 \exp(-1671.8/RT)$	L	Critical free volume
V_{fm}	0.025	L	Free volume of the monomer
a_m	0.001	L/K	Thermal expansion coeff. of the monomer
V_{fp}	0.025	L	Free volume of the polymer
a_p	0.00048	L/K	Thermal expansion coeff. of the polymer
m	0.5	-	Gel-effect model parameter
n	1.75	-	Gel-effect model parameter
A	0.348	-	Rate of decrease of k_t
k_3	$9.44 \exp(-3832.9/RT)$	-	Onset pt. of translational diffusion control
l_0	7.4×10^{-8}	cm	Length of monomer unit per chain
k_{th}	$1.35 \times 10^7 \exp(-27450/RT)$	$L^2/mol^2/min$	Thermal (self) initiation rate

Table 3: Kinetic Constants for Methyl Methacrylate

Parameter	Value	Unit	Description
M_w	100.12	g/mol	Molecular weight of the monomer
T_{gm}	167.1	K	Glass transition temp. of the monomer
T_{gp}	378	K	Glass transition temperature of the polymer
C_{pm}	411.1	cal/kg/K	Heat capacity of the monomer
C_{pp}	400	cal/kg/K	Heat capacity of the polymer
ΔH	-143.624	cal/mol	Heat of reaction
ρ_m	$0.9665 - 0.001164 \times (T - 273.15)$	kg/L	Density of the monomer
ρ_p	$1.195 - 0.00033 \times (T - 273.15)$	kg/L	Density of the polymer
k_p	$2.952 \times 10^7 \exp(-4353/RT)$	L/mol/min	Rate of propagation
k_t	$5.88 \times 10^9 \exp(-701/RT)$	L/mol/min	Rate of termination
$k_{td,ratio}$	$1.6093 \times \exp(-440.12/RT)$	-	Disproportionation to combination ratio
k_{fm}	$9.345 \times 10^4 \exp(-7475/RT)$	L/mol/min	Transfer to monomer rate
k_{fp}	0	L/mol/min	Transfer to polymer rate
k_{pin}	0	L/mol/min	Internal double bond rate of propagation
k_{pte}	0	L/mol/min	Terminal double bond rate of propagation
Δ	0.001	L/g	Reaction radius for segmental diffusion
V_{fc}	$0.7408 \exp(-1589.6/RT)$	L	Critical free volume
V_{fm}	0.025	L	Free volume of the monomer
a_m	0.001	L/K	Thermal expansion coeff. of the monomer
V_{fp}	0.025	L	Free volume of the polymer
a_p	0.00048	L/K	Thermal expansion coeff. of the polymer
m	0.5	-	Gel-effect model parameter
n	1.75	-	Gel-effect model parameter
A	1.11	-	Rate of decrease of k_t
k_3	$0.563 \exp(-8900/RT)$	-	Onset pt. of translational diffusion-control
l_0	6.9×10^{-8}	cm	Length of monomer unit per chain
k_{th}	$2.26 \times 10^{-8} \exp(-6578/RT)$	$L^2/mol^2/min$	Thermal (self) initiation rate